Supporting Information

A Robust Strategy Enabling Addressable Porous 3D Carbon-based Functional Nanomaterials in Miniaturized Systems

Nongnoot Wongkaew,[a]† Marcel Simsek,[a]† Palaniappan Arumugam,[b] Arne Behrent,[a] Sheela Berchmans[b] and Antje J. Baeumner[a]*

[a] Institute of Analytical Chemistry, Chemo- and Biosensors, University of Regensburg, 93053 Regensburg, Germany

[b] Council of Scientific and Industrial Research- Central Electrochemical Research Institute, Karaikudi, 630003, India

† These authors contributed equally to this work.

* Corresponding author: E-mail: antje.baeumner@ur.de

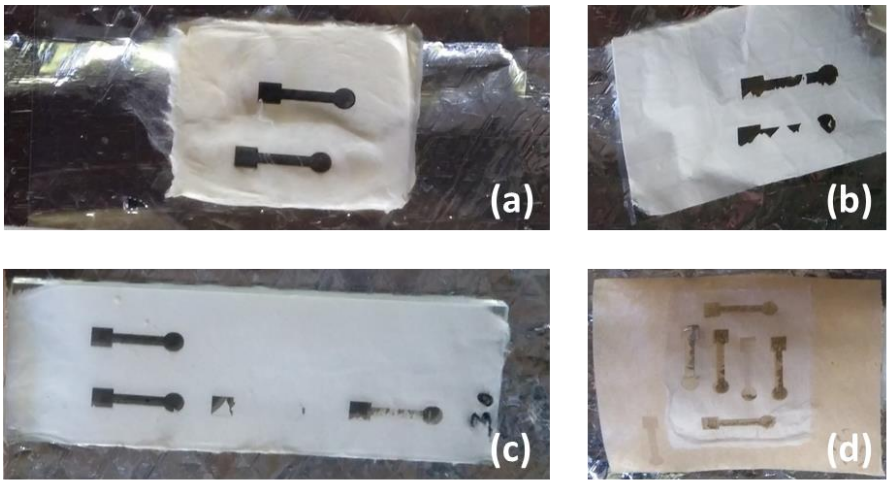

Figure S1. Preliminary investigation on finding out the proper substrate for collecting nanofibers. The photographs show the LCNF electrodes derived from Matrimid nanofiber mat electrospun on ITO sheet (a), aluminum foil (b), glass slide (c), and wax paper (d).

In comparison to the other substrates (Figure S1) such as glass slide, wax paper, and aluminum foil, ITO yields the best electrode feature for un-optimized lasing conditions.

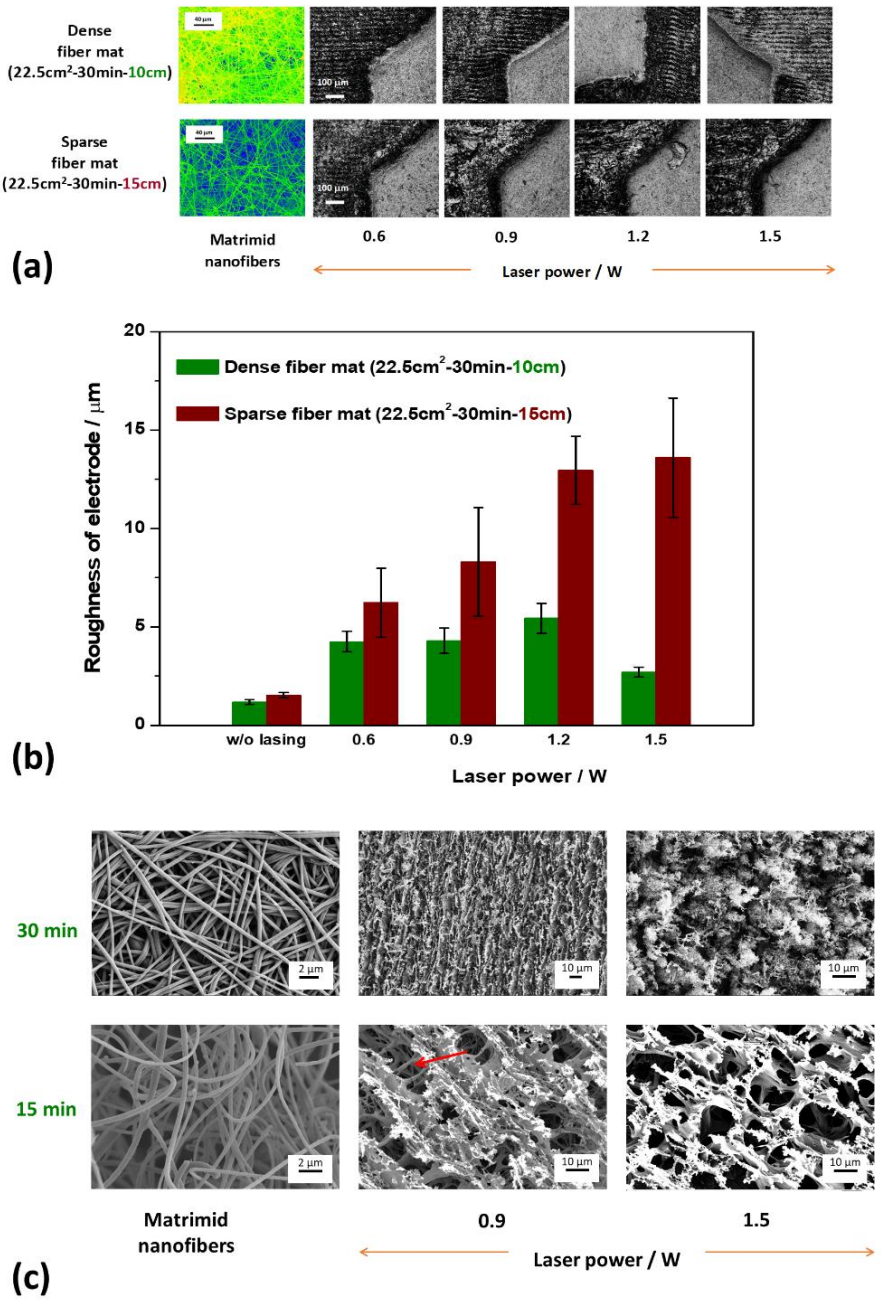

Figure S2. (a) Effect of fiber mat density spun at various settings (area-time-TCD) on macroscopic morphologies of LCNF electrode at various laser powers. (b) Quantification of the roughness of LCNFs shown in (a). (c) Effect of the electrospinning time on the

microscopic fiber morphology (TCD = 10 cm). The red arrow indicates the obtained fiber structures after laser-induced carbonization.

The morphology of the electrospun nanofiber mat with respect to its density can be controlled by the tip-to-collector distance (TCD) and collecting time. While sparse fiber mats feature larger pore sizes when compared to dense fiber mats, we found that too thin and sparse fiber mats derived from collecting fibers on a large collecting area (22.5 cm^2) and long TCD (15 cm) result in distorted and flaky electrodes as depicted in Figure S2a (lower panel). The electrode roughness increases with increasing laser power as determined by 3D-confocal laser microscopy (Figure S2b). In contrast, the roughness of the electrode derived from dense fiber mats (using 10 cm TCD, 30 min, 22.5 cm^2) does not change significantly with varying laser power conditions, and in fact is comparable to the density of non-scribed fibers. When fiber mats are spun too dense (30 min collecting time) SEM images reveal either a sheet-like structure or an irregular structure upon treatment with laser powers of 0.9 W and 1.5 W, respectively (Figure S2c-upper panel). Reducing the density (15 min collecting time) fibrous structures are retained (Figure S2c-lower panel). Hence, final electrode morphologies are easily tunable simply by controlling the electrospinning process, i.e. TCD, applied voltage, collecting area, feeding rate, etc.

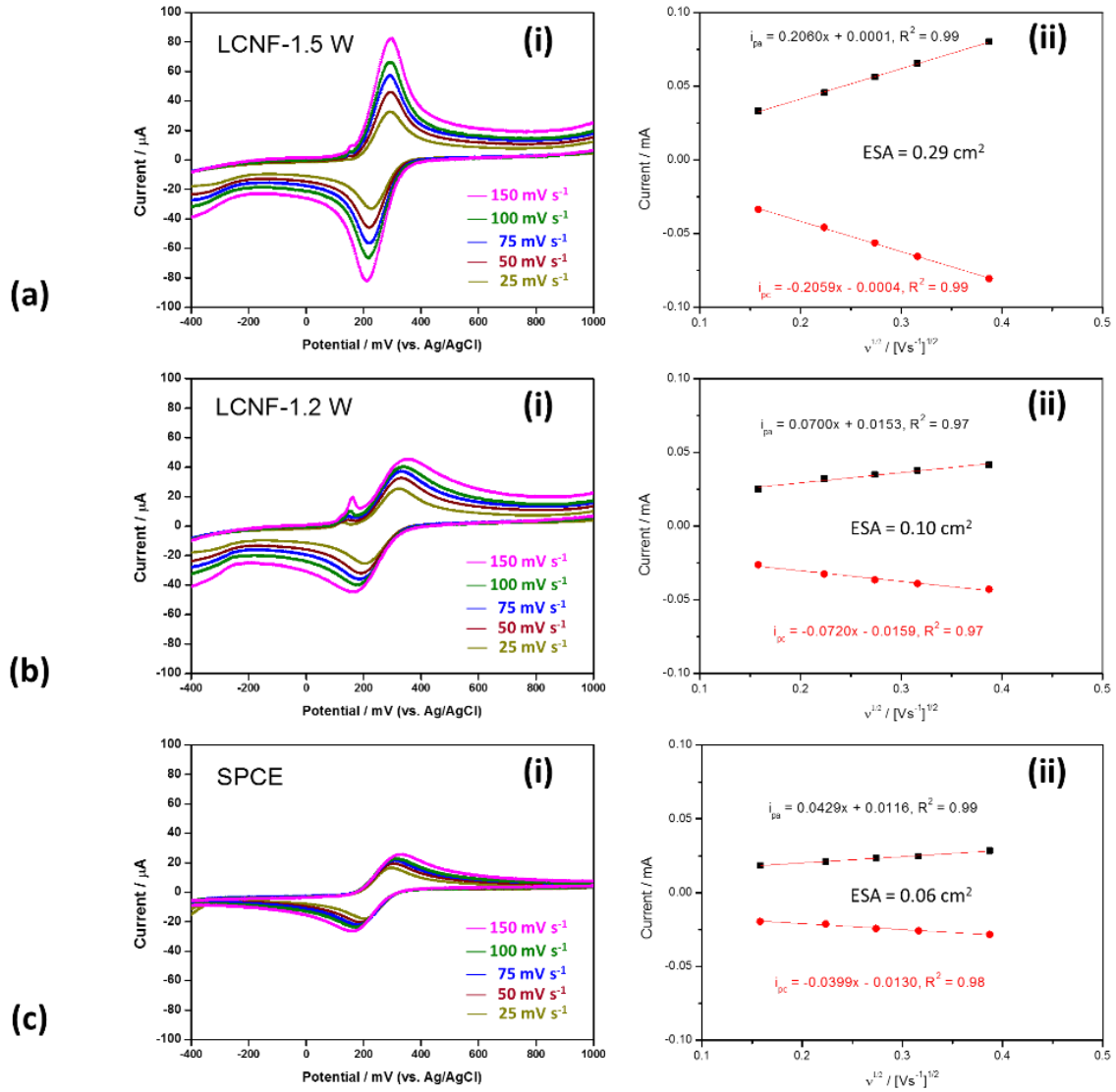

Figure S3. Panel (i): cyclic voltammograms at various scan rates for LCNF electrodes lased at 1.5 W (a), 1.2 W (b), and screen-printed carbon electrode (SPCE) run in 1 mM ferro/ferri cyanide (in 0.1 M phosphate buffer, pH 7.0, 0.1 M KCl). Panel (ii): Randles-Sevcik plots for the corresponding voltammograms in panel (i). Diameter of electrode was 3 mm^2. The nanofibers contained 3% iron.

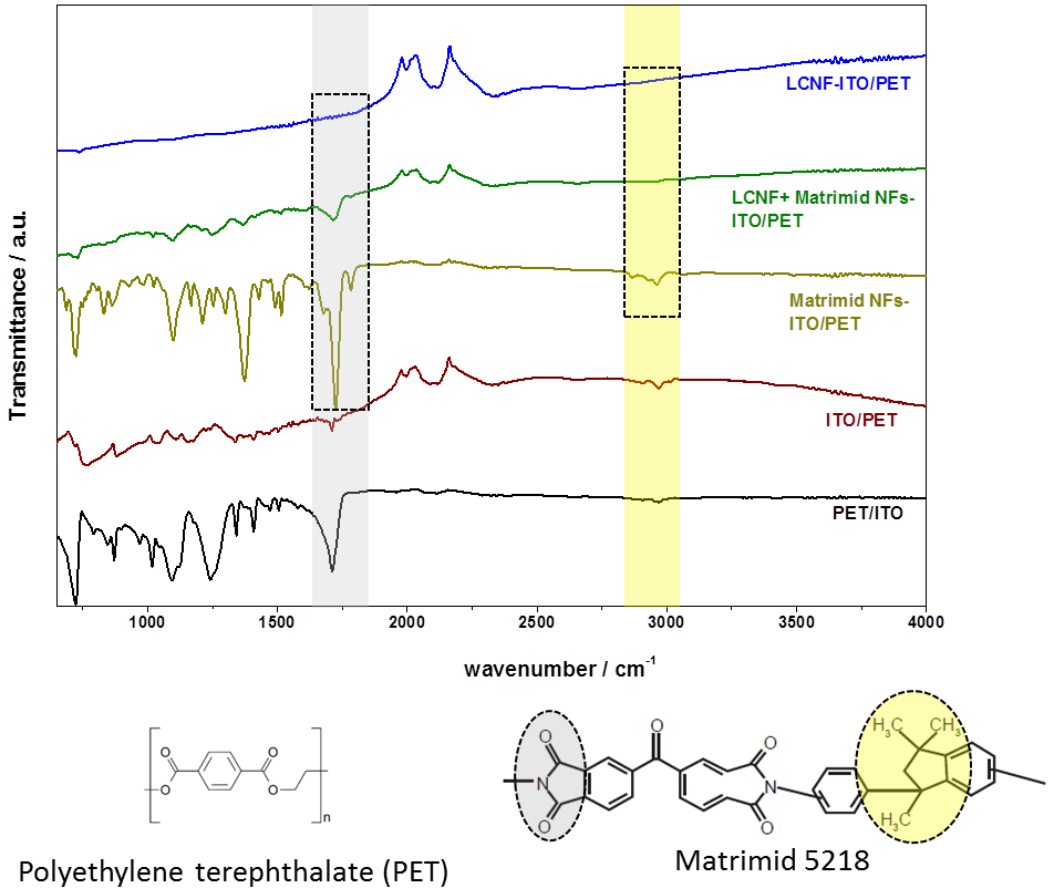

Figure S4. FTIR-ATR spectra of LCNF electrodes. LCNF + Matrimid NFs-ITO/PET was prepared from applying laser out-of-focus (-2mm) 30 times.

Table S1 Chemical compositions of Matrimid nanofibers and LCNFs containing 5% iron determined by elemental analysis (unless stated otherwise)

Sample	%				
	C	H	N	O	Fe
Matrimid nanofibers	73.6±0.4	4.6±0.1	4.9±0.1	16.1±0.5	0.75*
LCNFs	89.3±0.7	0.9±0.1	0.7±0.1	8.8±0.6	0.65±0.15**
% Change from initial content	↑ 21	↓ 80	↓ 85	↓ 45	-

* calculated theorectical value; ** evaluated from three different LCNF electrodes by X-ray photoelectron spectroscopy (XPS)

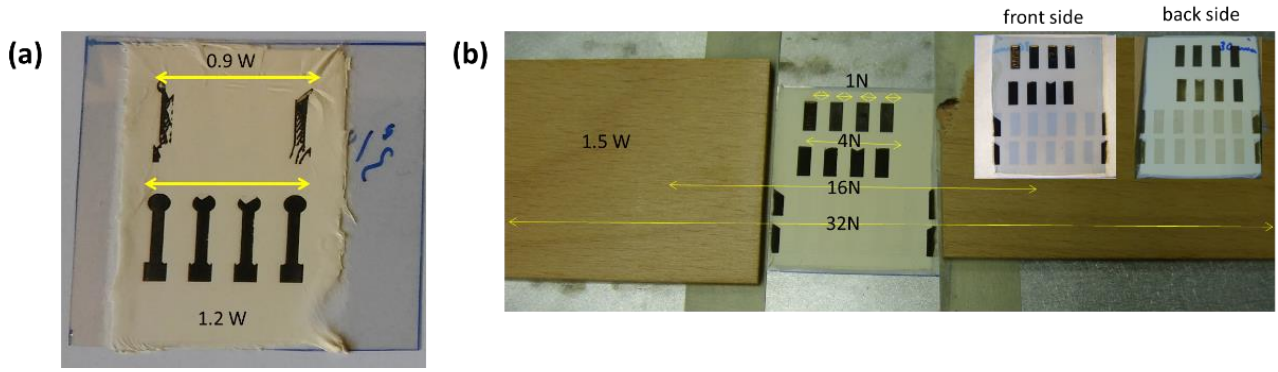

Figure S5. (a) Effect of laser power on LCNF fabrication (15 min-fiber mat). (b) Setup for lasing nanofiber mat with high number of electrode in a row (30 min-fiber mat). The photographs (inset) show the LCNF electrodes after scribing on the front- and back side. Matrimid nanofibers in (a) and (b) contain 3% and 5% iron, respectively.

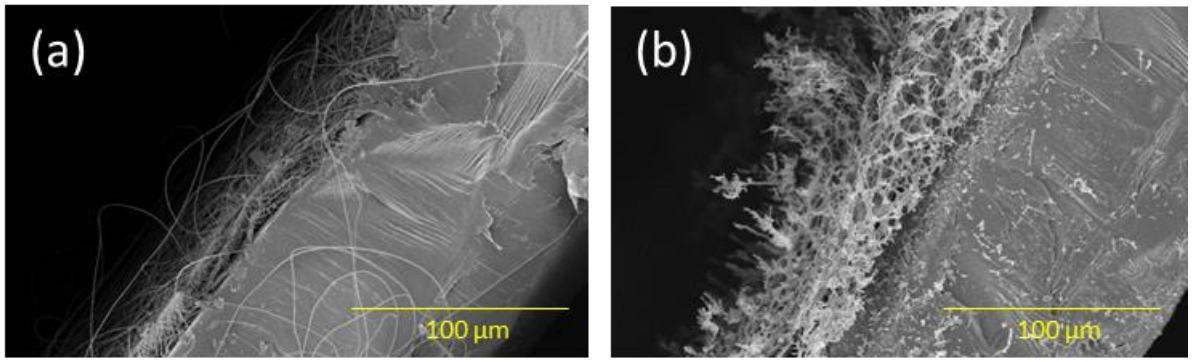

Figure S6. Side views of Matrimid nanofiber mats on ITO-PET substrate before (a), and after (b) laser carbonization.

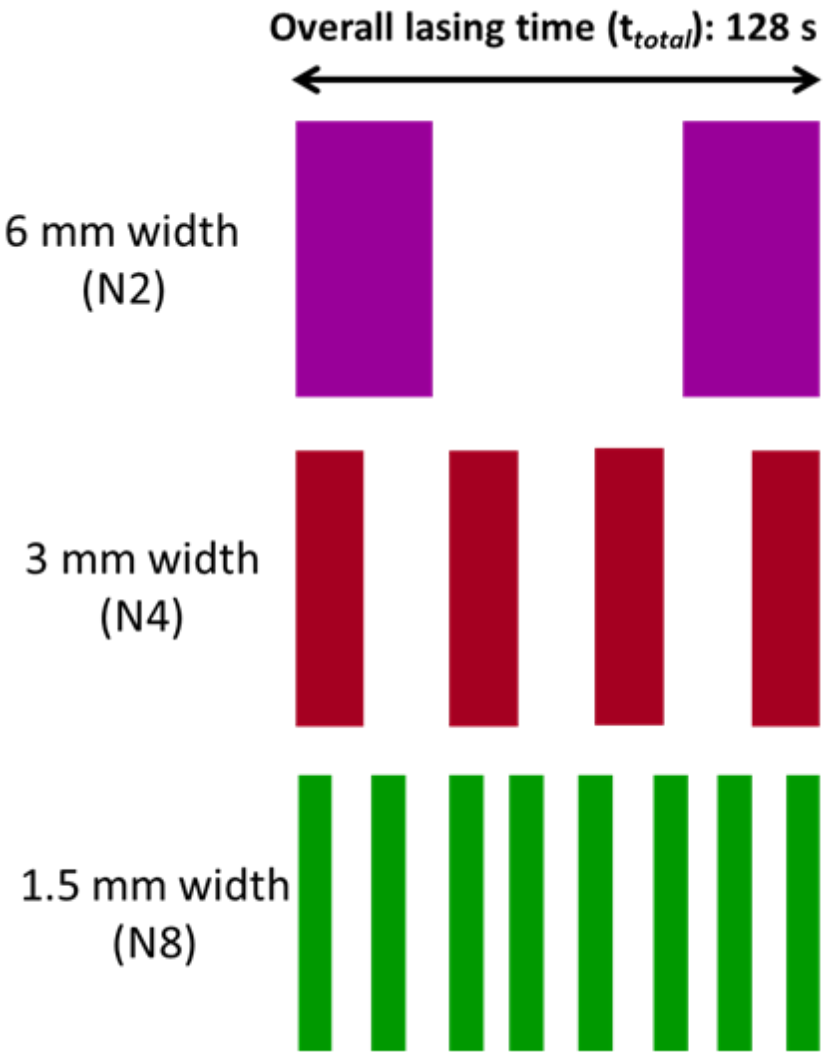

Figure S7. (a) The $t_{total}/t_{N(i)}$ of 15 per electrode was applied to the designs that consist of various electrode number and width while maintaining t_{total}. $t_{N(i)}$ for N2, N4 and N8 is ca. 1.08 s, 2.17 s, and 4.34 s, respectively

Table S2. Evaluation of cyclic voltammograms for 1 mM dopamine using various carbon-based electrodes (LCNF contained 5% iron)

Compared parameter	SPCE	LCNF	LCNF-UV/Ozone
ESA [cm^2] estimated from 1 mM ferrocyanide	0.06	0.12	not determined
E_{pa} [mV]	298	356	210
E_{pc} [mV]	92	98	160
Peak-to-peak separation [mV]	206	258	50
I_{pa} [µA]	10.78	17.40	45.76
I_{pc} [µA]	-3.613	-9.248	-17.43
Ah_{anodic} [Amp ×V]	0.8540	1.625	1.917
$Ah_{cathoodic}$ [Amp ×V]	0.4740	0.7812	0.7012

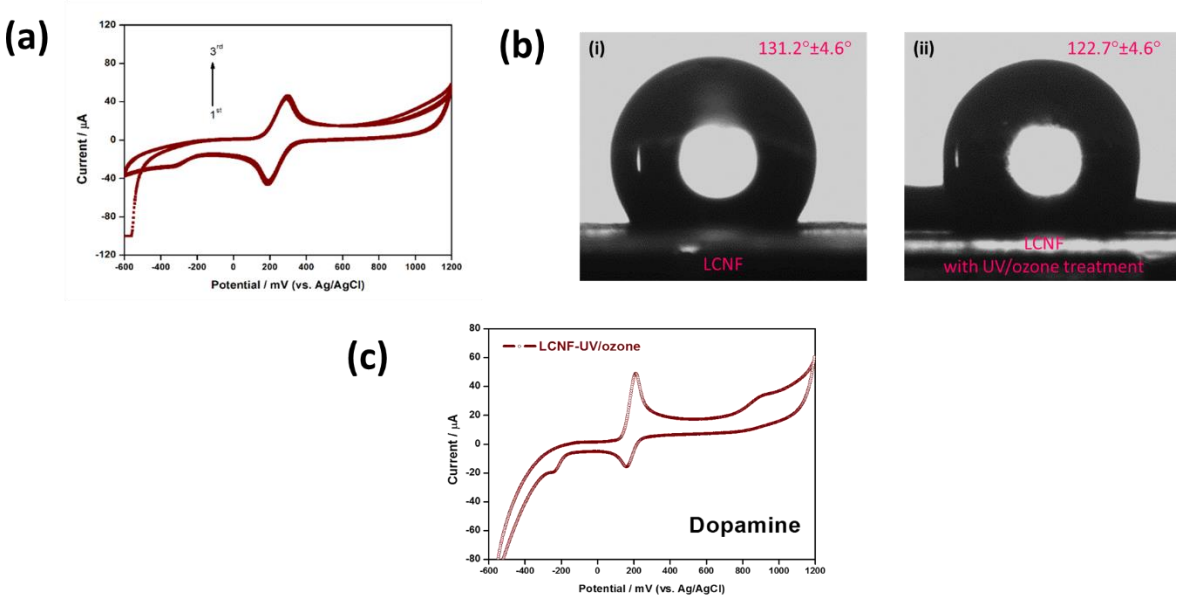

Figure S8. (a) Three cycles of cyclic voltammograms of 1 mM ferro/ferri cyanide from LCNF electrode treated with 1 min UV/ozone. The LCNF electrode was prepared from 5% iron nanofibers and lased at 1.5 W laser power with the speed of 762 mm s^{-1}. (b) Contact angles of (i) LCNF electrode, and (ii) UV/ozone-treated LCNF electrode. (c) Cyclic voltammogram of 1 mM dopamine using UV/ozone-treated LCNF electrode.